EXPERIMENTAL STUDY OF A COMPUTATIONAL HYBRID METHOD FOR THE RADIATED COUPLING MODELLING BETWEEN ELECTRONIC CIRCUITS AND ELECTRIC CABLE

Elagiri Ramalingam Rajkumar, Blaise Ravelo, Mohamed Bensetti, Yang Liu,
Priscilla Fernández López, Fabrice Duval and Moncef Kadi
IRSEEM-EA4353 at the Graduate School of Engineering ESIGELEC,
Av. Galilée, B.P. 10024, 76801 St Etienne du Rouvray, France.

ABSTRACT

In this paper, a computational hybrid method (HM) is developed for calculating the radiated coupling on an electric cable due to external electromagnetic (EM) near-field (NF) perturbations. These sources of EM perturbation are placed at some mm of the cable proximity. The analytical approach for evaluating the voltage across the cable extremities in function of the NF aggression is proposed. The HM proposed is based on the combination of analytical coupling models and numerical methods or measured data associated to calculate the induced voltages on the cable. The model developed is tested and validated for different configurations of the perturbing source in the wide frequency band from 200 MHz to 2 GHz. The methodology was validated with measurements comprised of two electric cables in different positions.

KEYWORDS: *Hybrid method (HM), near-field (NF) radiation, radiated emission, NF coupling, electromagnetic compatibility (EMC).*

I. INTRODUCTION

With the increase of the systems integration density as the modern automotive equipments, the electromagnetic compatibility (EMC) and electromagnetic interference (EMI) can be sources of serious problems to the electronic and electrical circuits [1-2]. Facing to these unintentional disturbing effects, standards on the testing techniques were established to ensure the safety of the automotives [3-6]. In addition, characterization methods of EMC and EMI prediction techniques were proposed [7-8]. One of the most difficult situations for the treatment of the EMC/EMI influences in the automotive systems concern the issues related to the immunity and the susceptibility of electronic circuits especially in radiating context [9-10]. To overcome these limitations, efficient methods are required. During the calculation of radiated coupling between electronic components and transmission lines, the active or passive components are usually represented by network of electric and/or magnetic dipoles [11-12]. This dipole set radiates the same EM fields as that of the any electronics component/integrated circuit. In EM coupling on cabling systems, the knowledge of exciting source is at least as important as modelling of cable network itself [13]. Due to the higher operating frequency of advanced electronic embedded systems in the automobile and aeronautical industry, the study of EMI between components and cables is an important topic of researcher. In this context, the non-uniform external exciting source is derived from the incident EM fields in the absence of the cable which is assumed as a transmission line (TL) displayed in Fig. 1.

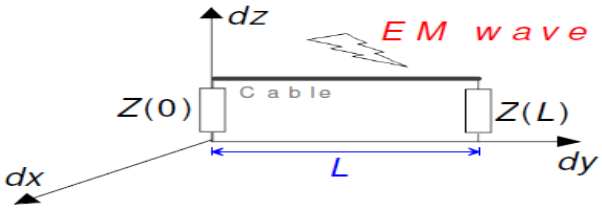

Figure 1. Configuration considered for investigating the coupling between a TL and NF EM radiations.

This is derived analytically in [14-18]. In this model, the coupling of the incident EM field on a TL is described by the application of a pair of per-unit-length current I_s and voltage generator V_s. In the particular case of transmission line above a ground plane, this model provides the induced voltage and current everywhere on the line.

But till now, few studies [17-18] were performed on the investigation of the EM NF coupling including the evanescent waves on the electric wires or cables. The existing ones are not valid for all cases of positions between the radiating structure and the victim wires. For this reason, we propose to experiment the HM (HM) whose the basic principle is introduced recently in [19-23]. For that, we will start with the analytical approach illustrating the functioning of this HM and then, we validate the concept with experimental studies. The paper will be ended by a conclusion.

II. METHODOLOGY OF THE HYBRID METHOD PROPOSED

As argued in [19-23], the HM developed in this paper is based on the combination of the given EM-data with the analytical modelling of the coupling voltages. As we are aimed to the computation of the voltage values in function of the operating frequency, we employ the Taylor modelling method [14] briefly described in the following paragraph.

2.1. Recall on the Taylor Model

For the better understanding, we consider the representation of the structure shown in Fig. 2. The infinitesimal elements with length *dy* can be assumed as its RLCG electrical model with per unit length parameters: R_u, L_u, C_u and G_u respectively expressing the resistance, inductance, capacitance and conductance per unit length. The appendix of this paper summarizes certain characteristics of the case of the TL formed by a cylindrical electric cable above the ground plane.

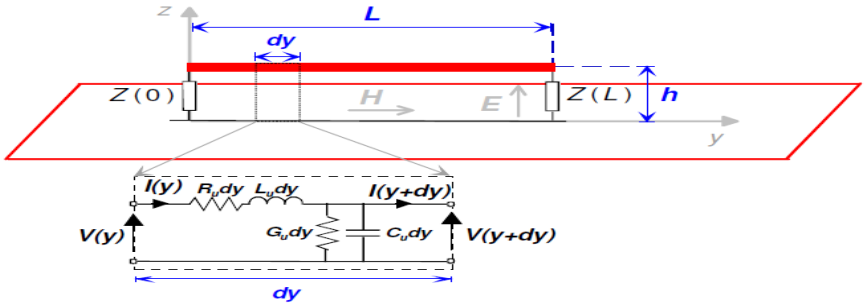

Figure 2: TL coupled with an electric field and its equivalent circuit.

We denote V_s the voltage derived from the transverse component of magnetic field in an elementary cell of the structure shown in Fig. 2 as:

$$V_s(j\omega) = j\omega \cdot h \cdot \mu_0 \cdot H_y . \quad (1)$$

where H_y represents the transverse component of the magnetic field and h is the height of the line. μ_0 is the magnetic permeability of vacuum; ω is the angular frequency given by $2\pi c/\lambda$ (c is the speed of the light in the vacuum). The current I_s is derived from the normal component of the incident electric field according to the relation:

$$I_s(j\omega) = j\omega \cdot C_u \cdot E_z . \quad (2)$$

where C_u represents the physical capacitance per unit length of the transmission line.

The transverse magnetic field and the normal electric field are supposed to be constant along the height of the line, considering that the source is a far-field source. The response of conductor TLs illuminated by an EM field has been reported by various investigators [17-18].

The model developed in [18] represents the effect of external EM NF field on a TL above a ground plane as a function of the exciting electric and magnetic fields. This analytical model is developed in the absence of TL and perturbation source is always placed above the TL. From the results between the modelled and coupled voltages, it is observed that this method is capable of analyzing when the perturbation source is placed above the line i.e. in the case of uniform field distribution. One major constraint of this model is that, when the perturbation source is placed between the line and the ground plane. This model is not considering the coupling between the cable and ground plane, and also the perturbation source and ground plane and the cable. Thus it is necessary to have a model which is capable of overcoming the above limitations. As illustrated in Fig. 3, the calculation of EM coupling due to uniform and non-uniform EM field is presented here. The relation between the total voltage and the current, as a function of the exciting EM field, is given by the following equations [14]:

$$\frac{dV(y)}{dy} + j\omega L_u I(y) = -j\omega\mu_0 \int_0^h H_y^e dz\,, \tag{3}$$

$$\frac{dI(y)}{dy} + j\omega C_u V(y) = -j\omega C_u \int_0^h E_z^e dz\,, \tag{4}$$

where superscript "*e*" refers the incident field of both magnetic and electric fields. We point out that the boundary conditions for a line terminated with impedances $Z_0 = Z(0)$ and $Z_L = Z(L)$ are given by:

$$V(0) = V_0 = -Z_0 I(0)\,, \tag{5}$$

$$V(L) = V_L = -Z_L I(L)\,. \tag{6}$$

These relations represent the equivalent Taylor model on coupling and its approach allows us to model the EM disturbance generated on the line, by a voltage source which represents the influence of transverse magnetic field $H_y(y,z)$ and a current source which represents the influence of the vertical electric field $E_z(y,z)$ distributed along this line.

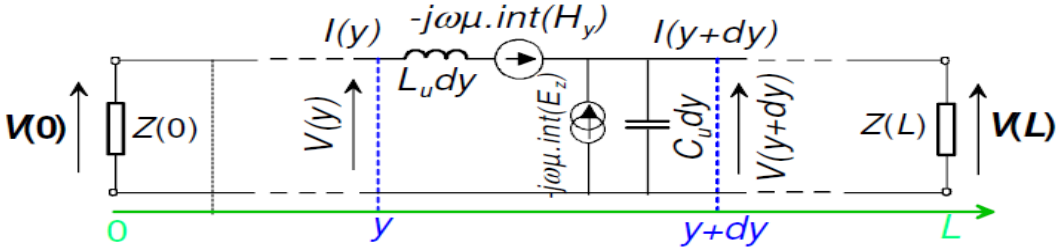

Figure 3. Representation of the Taylor model.

The existing models that are based on analytical expressions calculate the induced voltage for cases when the TL is excited by a plane wave. The numerical methods as finite element method (FEM) and finite integral technique (FIT) require high computational resources and longer duration in simulation and analytical methods are bound to be in transverse EM quasi-static conditions. Thus, the HM capable of predicting and calculating the induced voltages and currents, will be the solution for determining the induced voltages in the near-field analysis.

2.2. HM Formulation

In the calculation of radiated coupling with analytical model, normally in the calculation of E and H field, we used to consider the total field to obtain the complete radiated field, whereas in the case of analytical method we are not obliged to include the scattering field due to the fact that the model is considered in the absence of the cable and also with the ground plane condition. This calculation also incepts the image theory concept for the sake of ground plane condition. Added to that, this method is not valid when the cable is very nearer to the perturbation source. This model is capable of analyzing the coupling with the field is uniform and not with non uniform field. Whereas in the real time industrial conditions, are dealt with non uniform field also and very close to the perturbation source.

These limitations posed by the purely analytical models lead us to find a solution to overcome the above limitations.

In our work, we utilize the quasi-static condition while formulating the setup. Hence, the HM which is capable of handling these situations has been illustrated in the flow analysis of Fig. 4. This solution is limited to electrically short ($L < \lambda$) and matched TLs ($Z_0 = Z_L = Z_C$). Equations (3)-(4) and (5)-(6) thus become:

$$V_s(j\omega) \cdot L = -j\omega \cdot \mu_0 \cdot A \cdot H_y^e, \quad (7)$$

$$I_s(j\omega) \cdot L = -j\omega \cdot C_u \cdot A \cdot E_z^e, \quad (8)$$

where, $A = h \cdot L$ is the area between the centre of the line and the ground plane., E_z^e is the exciting, incident transverse electric field, μ_0 is the magnetic permeability of vacuum, H_y^e is the exciting, normal incident magnetic field.

The fields E_z^e and H_y^e are obtained by the FEM simulations in the presence of cable and the ground plane. This simplification is applied to an entire TL, not just an infinitesimal element *dy*. Thus, the simplified equivalent circuit of a TL can be represented as in Fig. 2. In this case, the voltage induced across the load Z_0 and Z_L by an exciting, EM incident field is given by:

$$V_0 = \frac{Z_0 L}{Z_0 + Z_L}(V_s - Z_L I_s), \quad (9)$$

$$V_L = \frac{-Z_0 L}{Z_0 + Z_L}(V_s + Z_L I_s). \quad (10)$$

As stated earlier, the HM proposed considers all the coupling phenomena: cable-dipole, dipole-ground plane and cable-ground plane. Another advantage of this method is the incorporation of the dipole based model in the radiated coupling calculation. From literatures, it is understood that plane wave excitation is widely used as incident EM field illumination. The work demonstrated in [17-18] has the limitations, when the radiating source is placed very nearer to the cable (victim).

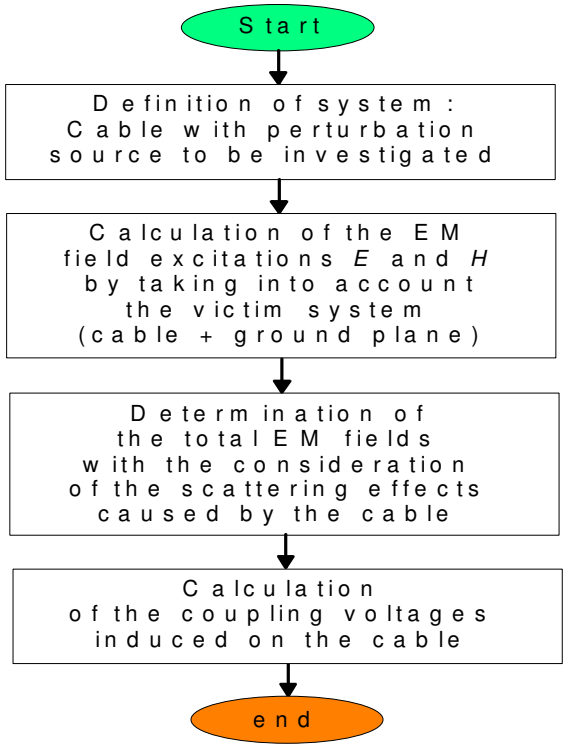

Figure 4. Flow analysis of the HM proposed.

Hence, this method considers the limitation posed by the previous works and the calculation of the mean value integration is replaced by the integral calculation of each and every mesh from the centre point of each element of the mesh. Subsequently, equations (7) and (8) are transformed as follows:

$$V_s L = -j\omega\mu_0 \sum_{\Delta y}\sum_{\Delta z} H_y^e \Delta y \Delta z \,, \tag{11}$$

$$I_s L = -j\omega\mu_0 \sum_{\Delta y}\sum_{\Delta z} E_z^e \Delta y \Delta z \,. \tag{12}$$

The discrete values of the meshes Δy and Δz are illustrated in the following section.

To verify the relevance of this theoretic approach, numerical experiments were carried out by using the scientific tool Matlab programs.

2.3. Application Examples

As depicted in Fig. 5(a), an electric wire with radius $r_0 = 0.1$ mm and length $L = 8$ mm above a ground plane at a height of $h = 2$ mm is used as the target device and an elementary electric dipole placed randomly and the ground plane and the wire is used as the radiating source. Both the terminals of the wire are terminated with matched 221 Ω impedance. The dipoles are excited by a current of $I_0 = 0.2$ A throughout the study and this is being tested with various configurations. Two different cases of the radiating sources position (D_1 and D_2 are placed respectively above and below the cable) were analyzed. The mathematical expressions of EM field radiation are indicated in [24-25].

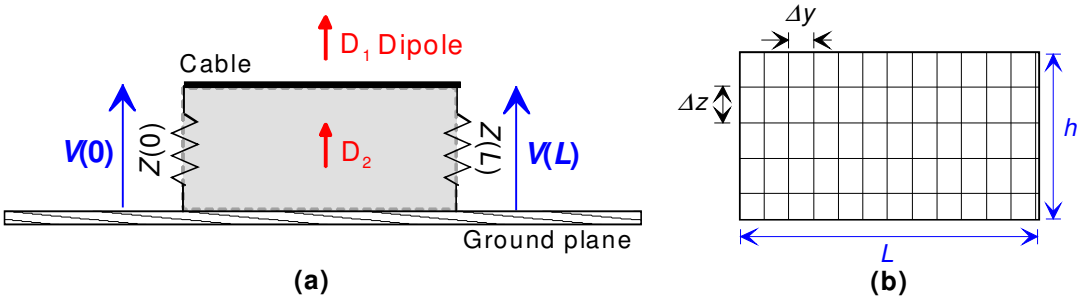

Figure 5. (a) Cable loaded by $Z(0) = Z(L) = 221\Omega$ and radiating dipoles D_1 above and D_2 below the ground plane. (b) Mesh of the surface plane for calculating the coupling voltages.

Fig. 5(b) represents the illustration of the meshing in the shadowed surface for calculating the coupling voltages. The EM field values E_z and H_y are determined by FEM simulation and substituted equations (11)-(12) in equations (9)-(10) to obtain the coupled voltage V_0 and V_L.

Fig. 6(a) presents the comparisons of voltages at the extremities of the cables caused by the EM couplings for the case of dipole D_1 positioned at 1 mm above the cable. We can see that the results obtained by the HM, the results show good accordance with each other in very wide microwave frequency band from 0.2 GHz to 2.0 GHz. It is evident that thanks to the consideration of all coupling effects of the system, this HM achieves better correlation in calculation of the induced voltages; with about relative errors lower than 3 % from the results in Fig. 6(a).

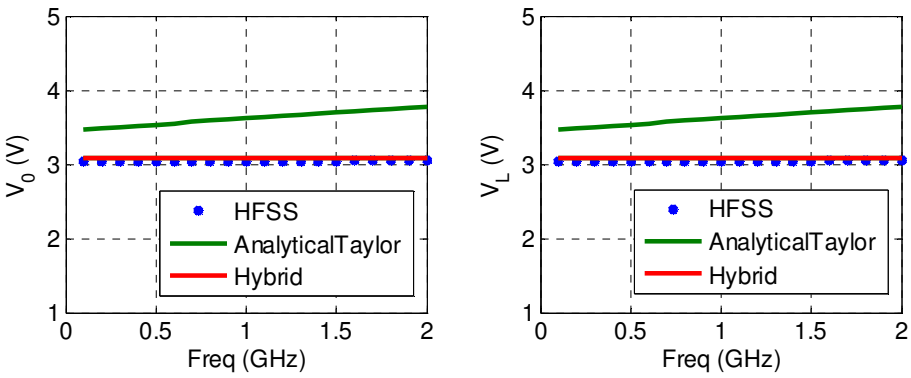

Figure 6(a). Flow analysis of the HM proposed.

In complementary to the previous case, we also investigated the effectiveness of the method proposed by placing the dipole radiating source at 1 mm below the cable as depicted in Fig. 5(a) only with the dipole D_2. Once again, as explained in Fig. 6(b), we observe that a very good agreement between the HM results and those form the FEM full wave computation carried out with HFSS and the pure analytical one using the Taylor formula. With these results, we assess relative errors lower than 2 %. Hence, we understand that it is possible to investigate the perturbation source near the cable for various frequency ranges from 200 MHz up to 2 GHz. In the calculation of induced voltages due to perturbation source in the same plane of components and cables, this method can be used to obtain the required electrical components.

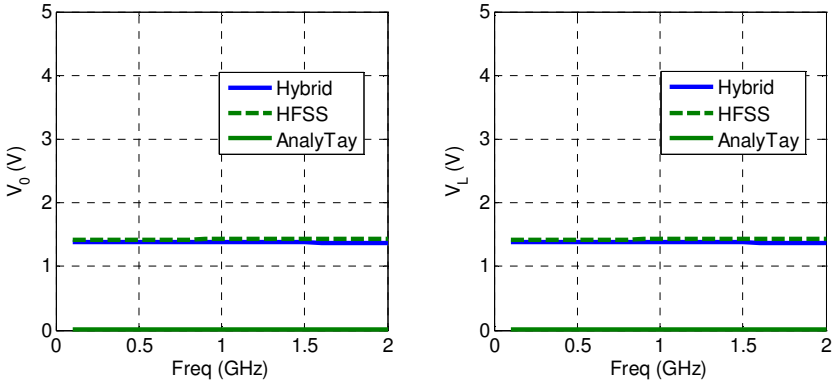

Figure 6(b). Comparison results from the HM, analytical calculation and HFSS simulations by considering the dipole element under the cable as shown in Fig. 5(a).

III. EXPERIMENTAL INVESTIGATION: COUPLING BETWEEN TWO ELECTRIC CABLES

To check the relevance of the HM methodology described in the previous section, experimental analyses were performed with design of electronic structures showing the influence of NF radiations interacting with a electric wire.

3.1. Design of the Structure Under Test (SUT)

As proof of concepts, we propose to evaluate the coupling voltages between the cables presented by the HFSS design shown in Figs. 7. To calculate the coupling between the perturbation source and electric wire, we use the electric wire (L = = 30mm, r = 0.4mm, h = 20mm).

As illustrated by Fig. 7(a), the source cable is kept at the reference position (-15mm, 0mm, 0.7mm) in the x-axis with radius, r = 0.5mm and length L = 30mm. The victim is kept at (-15mm, 5mm, 20mm) in the same x axis with the same dimensions of radius, r = 0.5mm and length L = 30mm. The simulation rectangular box is fixed at the reference position defined by (-52mm, -52mm, 0mm) and with the geometrical dimensions L_x = 104mm, L_y = 104mm and L_z = 30mm. To refine the mesh precision, we included the mesh box at (-16mm, 1mm, 0mm) and = 32mm, L_y = 3mm and L_z = 22mm with 1mm maximum length elements.

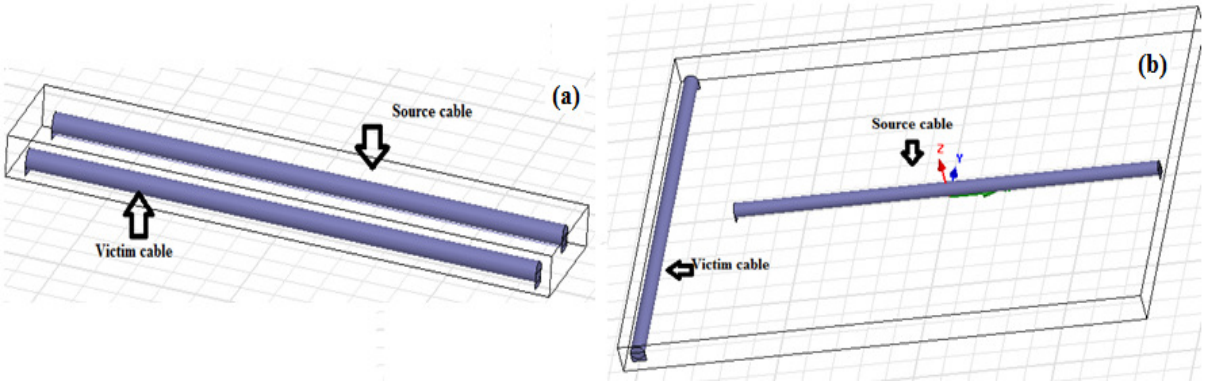

Figure 7. 3D HFSS design of the cables (a) in parallel and (b) in perpendicular configurations.

Fig. 7(b) describes the second case of the configuration cable with two cables in perpendicular position. In this case, the source cable is kept at the reference position (-15mm, 0mm, 0.7mm) in the x-axis with radius, r = 0.5mm and length L = = 30mm. The victim with the same geometrical dimensions is kept at (-20mm, -15mm, 20mm) in the same x-axis. The simulation rectangular box is fixed at the reference position of (-52mm,-52mm, 0mm) and L_x = 104mm, L_y = 104mm and L_z = 25mm. In this case, to refine the mesh precision we included the mesh box at (-21mm, -16mm, 0mm) and L_x = 37 mm, L_y = 32mm and L_z = 22mm with 1mm maximum length elements. The first setup both are in x-plane and later is having victim at the y-plane.
The simulations of the structures shown in Figs. 7 were carried over the frequency range between 0.5GHz to 3GHz and obtained the induced voltages at the terminations. In both configurations, the power is injected at the lumped port and is kept as 1mW.

3.2. Description of the NF Test Bench Used

Fig. 8 depicts the photograph of the experimental setup which includes the fabricated devices tested for scanning the EM NF of the IRSEEM laboratory. The radiating structure is comprised of a electric wire placed above a electric ground plane. With the experimentation, we are aimed to the analysis of the configuration with the following geometrical parameters: distance between the wires fixed to 30 mm, r = 0.4 mm, h_1 = 20 mm, L = 30mm and w = 40mm.

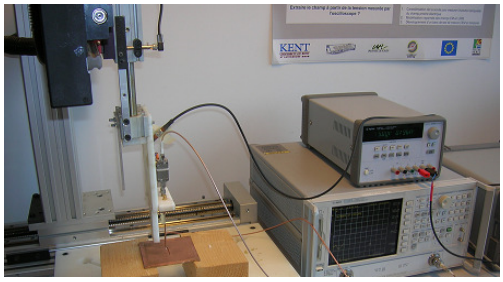

Figure 8. Experimental setup of the NF scan radiated by the cable source.

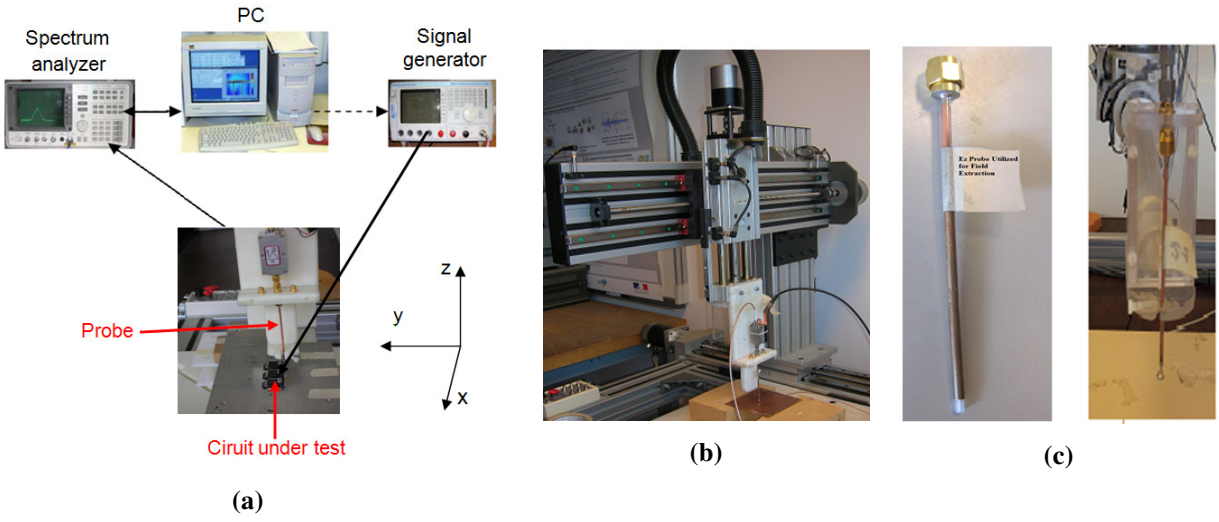

Figure 9. (a) Synoptic of the experimental setup. Photographs of (b) the robot and (c) the probes used.

We considered the synoptic of the experimental setup presented in Fig. 9(a). The EM NF radiated by the perturbation structure is detected from the electronic EM probes then recorded with a network analyzer. The probes shown in Fig. 9(c) are fixed at the arm of the robot photographed in Fig. 9(b). We point out that the radiating structure can be either excited by a signal synthesizer or directly with the network analyser and then the transmission parameters are exploited to determine the value of the radiated EM NF.

As argued before, this structure is considered as the source of the radiation and the second wire of same dimension placed in arbitrary position in the proximity of this source is supposed as perturbation source. The perturbation source is powered by the sine wave signal with input power P_{in} = -10dBm. The measurement was made by using the network analyzer programmed with 201 points. Then, we extracted the E_z and H_y fields for calculating the coupling.
For the first configuration, the victim is kept at 5mm distance from the source; the fields E_z and H_y are extracted. H_y is extracted from -15 mm to 15 mm with the step size of 1 mm and similarly E_z is extracted from 0 mm to 19.5 mm with the step size of 1 mm.

3.3. Calibrations Process

During the test, the lines are loaded with Z_0 = 200Ω. The disturbing line is fed by the sine wave voltages. Fig. 10(a) and Fig. 10(b) represent the models of the probes for scanning the EM NF radiated by the disturbing cable. The scan was made with electronic probes and recorded with a vector network analyzer. To increase the level of the voltage corresponding to the EM field detected, a broadband amplifier with 15 V power supply was used.

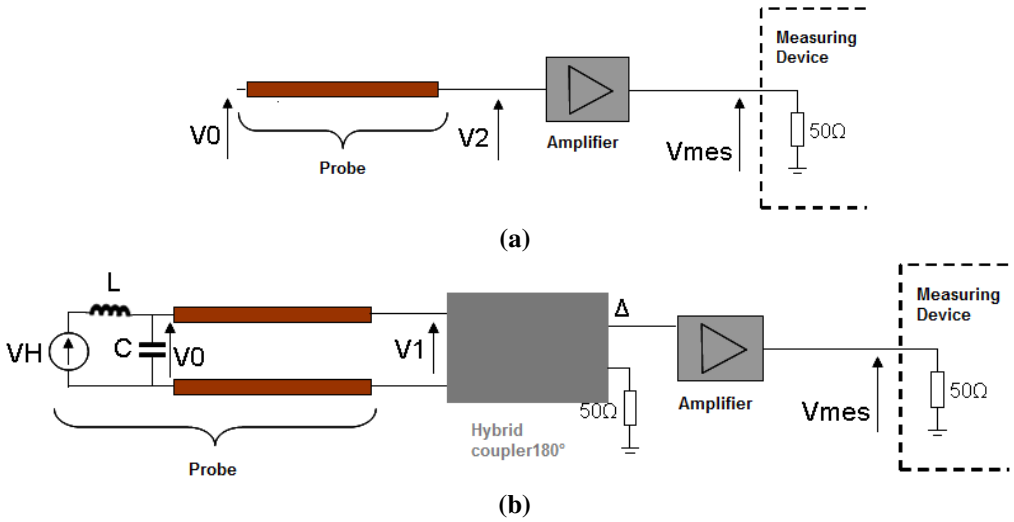

Figure 10. Electrical models of the (a) electric and (b) magnetic probes shown in Fig. 9(c) during the NF scan.

To measure the emitted field, we use successively several sensitive probes each in a certain constituent of the electric field component E_z and magnetic field component H_x. Probes are placed on the arm of the robot shown in Fig. 9(b) which, commanded (ordered) by a PC, moves them over the SUT. The PC assures the movement of the robot and makes the acquisition of the data measured by a vector network analyzer (VNA) Agilent 50713 operating between 100 kHz and 8.5 GHz. These data are converted in electric and magnetic fields (amplitude and phase) thanks to a grading of probes which we present in the following paragraphs.
From the measured transmission parameter represented by the complex data S_{21}, the extraction of the EM fields with the probes used (presented in Fig. 9(b)) during the test was performed thanks to the following expressions:

$$H_{xy} = a_{H_{xy}} V_{mes}(H_{xy}), \tag{13}$$

$$E_z = a_{E_z} V_{mes}(E_z), \tag{14}$$

with

$$a_{H_{xy}} = \frac{H_{xy}}{V'_{H_{xy}}}, \tag{15}$$

$$a_{E_z} = \frac{E_z}{V'_{E_z}}, \tag{16}$$

$$V_{mes} = |S_{21}|^2 e^{-j2\angle S_{21}} \sqrt{2 \cdot 10^{P_{indB}/10} \cdot Z_0}\,. \tag{17}$$

To extract the measured E_z, the procedure of measurement of the normal constituent E_z was taken into account by deeming the equivalent model depicted in Fig. 10(a). It consists of the probe monopole connected to the port of beginning of the amplifier. The output of the amplifier is connected to the measuring device. In that case, the factor to be determined is b ($E_z = b.V_{mes}$). It is also calculated by means of a circuit the theoretical brilliance of which we know ($b = E_{z\_theoretical}/V'_{mes}$).
To determine H_x, the procedure of measurement shown in Fig. 10(b) was considered. It contains the probe curl differential connected to the ports of beginning of the hybrid coupler 180 °. The output of the coupler is connected to the amplifier as highlighted by Figs. 10. The output of this one is connected to the measuring device. In practice, analyzing can be made by following the same methodology as for the electric field. However in the case of probes magnetic field, it is possible to model simply the buckle by means of discrete elements, and we are going to find the factor of the procedure by electric simulations performed with the electronic/microwave software ADS (Advanced Design System) from Agilent™.
To obtain the antenna factors of the various probes, we measure fields in 2mm over the cable pictured in Fig. 11, in 100MHz and in 3GHz (frequencies of our circuit tests) and we calculate the theoretical radiation in 2mm. We can see that the radiating device is a cylindrical wire with radius a = 1.5 mm placed at the height h = 2.05 mm above the ground plane.

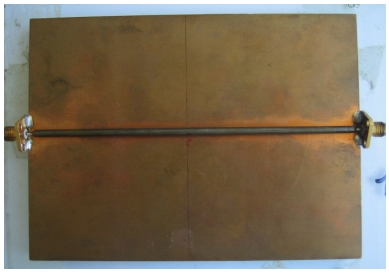

Figure 11. Photograph of the referential device for the calibration factor validation.

The geometrical representation is shown in Fig. A.1 of Appendix A. For the theoretical reference, we exploit the analytical expressions of the EM fields.

3.4. Experimental Results

By using the scanned EM NF, we evaluated the coupling on any wires placed at the proximity of this radiating structure via the HM understudy. To validate the results, comparisons with the simulations performed with HFSS were performed. So, two positions of the victim wires with the same length L = 30 mm presented with the perspective views of Figs. 7 were investigated.
Fig. 12(a) and Fig. 12(b) represent the maps of the modulus and phases of the measured EM NF from the scan of the structures shown in Fig. 8. These results correspond to the radiation of the experimented configuration at the operating frequency 3 GHz.

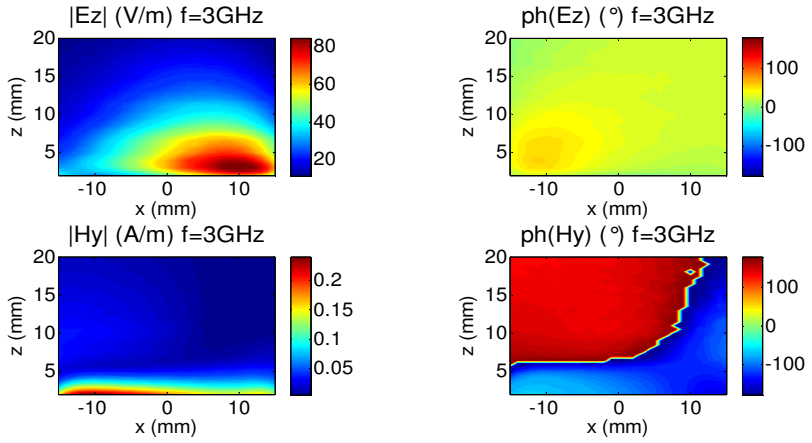

(a)

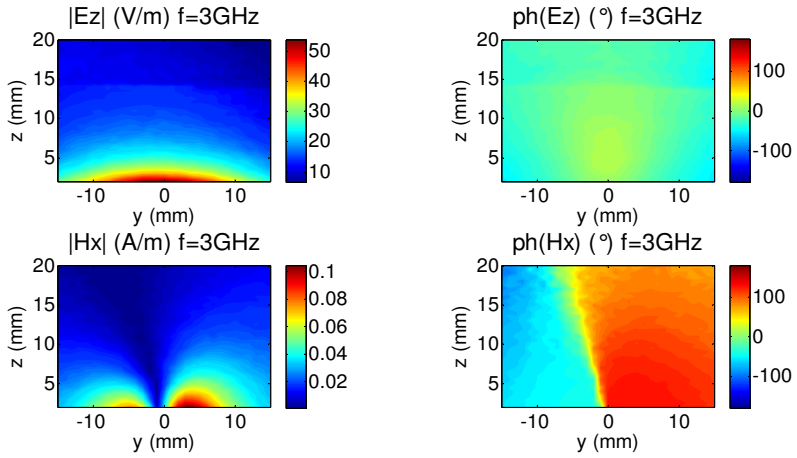

(b)

Figure 12. Maps of the measured electric and magnetic NF radiated by the SUTs corresponding to the configurations respectively shown in Fig. 7(a) and Fig. 7(b).

This EM NF data was scanned in the vertical surface plane defined by the fictive victim cable and the ground plane as illustrated in Fig. 5(a). To verify the relevance of the measured data, comparison with the EM NF from the measurement and theory described in the Appendix was also carried out during the calibration and the data processing. The profiles of Fig. 13 present the results obtained.

After the calculations with the standard scientific tool Matlab, we obtain the coupling voltages indicated in Table 1. This later addresses the comparison of results calculated from the HM under investigation and those computed with the full wave numerical method from HFSS with the configuration of Fig. 7(a). Table 2 represents the comparison between the HFSS and HM developed from 0.5 GHz to 3.0 GHz. Though the results are not in the good accordance each other, it is inevitable that the induced voltages increase as the frequency increases.

It is worth noting that the coupling effect calculation HM developed in this paper main presents many advantages as the flexibility with various complex structures, the wideness of the operating frequency band and its less computation time compared to the full wave tools.

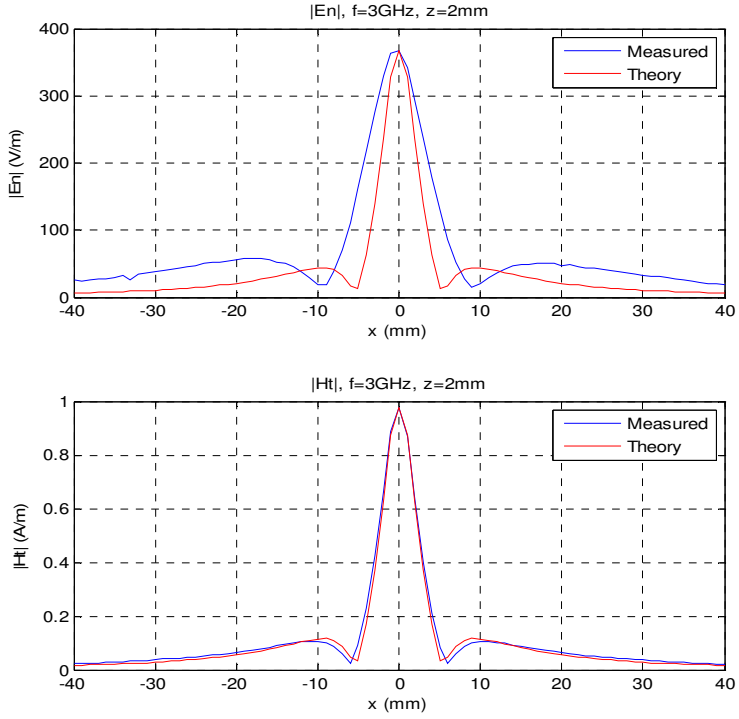

Figure 13. Comparison between the profiles of measured and theoretical electric and magnetic NF (H_t=H_y and E_n=E_z) of the structure corresponding to the configuration of Fig. 8.

Table 1. Comparison of the coupling voltages determined from HM measured computation and the full wave techniques with the configuration of Fig. 7(a).

Cables parallel	HFSS		HM (measurement)	
	V_0 (µV)	V_L (µV)	V_0 (µV)	V_L (µV)
0.5GHz	700	700	200	200
1GHz	800	800	300	300
1.5GHz	900	900	500	500
2GHz	1200	1200	600	600
2.5GHz	1300	1300	700	700
3GHz	1100	1100	900	900

Table 2. Comparison of the coupling voltages determined from HM measured computation and the full wave techniques with the configuration of Fig. 7(b).

Cables perpendicular	HFSS		HM (measurement)	
	V_0 (µV)	V_L (µV)	V_0 (µV)	V_L (µV)
0.5GHz	85	85	341	341
1GHz	800	800	684	684
1.5GHz	900	900	1020	1020
2GHz	1200	1200	1360	1360
2.5GHz	1300	1300	1710	1710
3GHz	1100	1100	2100	2100

IV. CONCLUSIONS

A HM dedicating to the calculation of NF EM coupling between the electronic components and electric cables is investigated. This HM is based on the association of the Taylor model and any numerical methods for determining the electrical field radiated by electronic structure from some hundreds MHz to some GHz. The analytical relations illustrating the different steps of the method are proposed. The results obtained using the HM proposed are promising for the calculation of radiated coupling. With the consideration of all the coupling phenomena, the coupling model was validated for various cases. This computational method can be utilized for the development of EMC and EMI standard method to predict and estimate the radiated coupling between complex electronic systems, for example, in automotive and aeronautical applications.

APPENDIX: THEORY OF THE ELECTRIC CABLE EM RADIATIONS

In order to study the coupling between the metallic cable and the ground plane, it is necessary to understand the cable characteristics by using the transmission line (TL) and its influences. The cable is constituted of cylindrical conductor representing the electric cable with *a*-radius placed at distance *h* above a ground plane as shown in Fig. A.1. This plane is situated in the horizontal (*Oxy*) plane of the rectangular 3D-(*Oxyz*).

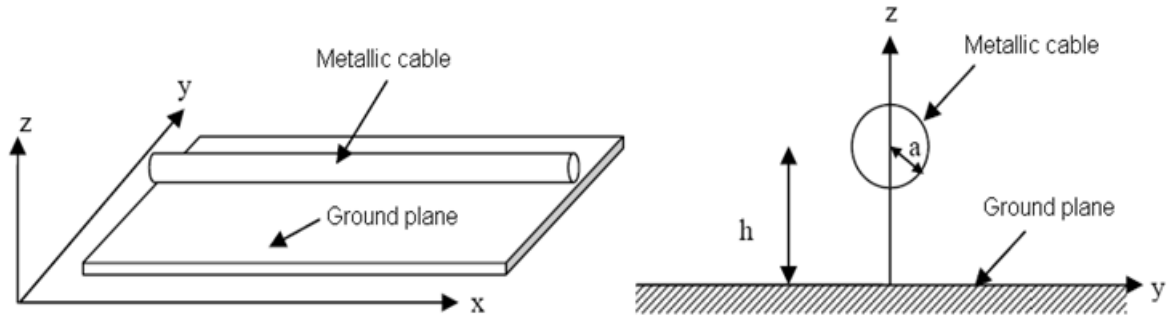

Fig. A.1: Cylindrical conductor with a ground plane. 3D view (in left) and view in (Oyz) plane.

A.1. Per Unit Length Parameters and Propagation Characteristics of the Electric Cable

Then, if the loss of the conductor cable is neglected, this structure presents an equivalent per unit length inductance and capacitance is given by:

$$L_u = \frac{\mu_0}{2\pi}\ln\left(\frac{2d}{a}\right), \tag{A-1}$$

$$C_u = \frac{2\pi\varepsilon_0}{\ln\left(\frac{2d}{a}\right)}. \tag{A-2}$$

Then, at the operating frequency *f*, the propagation constant is expressed as:

$$\gamma = j\beta, \tag{A-3}$$

where the phase constant is defined as:

$$\beta = \omega\sqrt{L_u C_u} = 2\pi f\sqrt{\varepsilon_0\mu_0}. \tag{A-4}$$

It was shown that the characteristic impedance associated to this TL is written as:

$$Z_c = \frac{1}{2\pi}\sqrt{\frac{\mu_0}{\varepsilon_0}}\cosh^{-1}\left(\frac{h}{a}\right). \tag{A-5}$$

The study of susceptibility of the cable is being associated with the radiated source; the radiated source in this study is the electrical dipole, which is made as the equivalent for the electronic component emission.

A.2. Recall on the Wave Propagation Theory

According to the wave propagation theory, we can formulate the travelling wave voltage written as:

$$V(z) = V_0^+ e^{-\gamma z} + V_0^- e^{\gamma z}. \tag{A-6}$$

The current of the wave propagation is given by:

$$I(z) = I_0^+ e^{-\gamma z} + I_0^- e^{\gamma z}, \tag{A-7}$$

and the complex propagation constant is:

$$\gamma = \alpha + j\beta = \sqrt{(R + j\omega L)(G + j\omega C)}, \tag{A-8}$$

where $e^{-\gamma z}$ term indicates the wave propagation in the positive *z* direction, and $e^{\gamma z}$ term indicates the wave propagation in the negative *z* direction. α is the attenuation constant. β is the phase constant. γ is the propagation constant. The characteristic impedance of the cable is defined as:

$$Z_c = \sqrt{\frac{R + j\omega L}{G + j\omega C}}, \tag{A-9}$$

The wavelength of the wave propagating along the line, which can be determined from the phase constant in equation (A-8), is set as:

$$\lambda = \frac{2\pi}{\beta}, \tag{A-10}$$

and the phase velocity is written as:

$$v_p = \frac{\omega}{\beta} = \lambda \cdot f, \tag{A-11}$$

where *f* is the frequency.

In general, when we are designing or simulating a transmission line, we assume that the transmission line is ideal. This means that there is no loss effect. Therefore, the loss of the line is very small and so can be neglected, by setting the resistance and conductance to zero. This results in the fact that the attenuation constant (α) is zero. Consequently, the characteristic impedance given in (A-9) becomes:

$$Z_c = \sqrt{\frac{L}{C}}, \tag{A-12}$$

The wavelength defined in (A-10) is transformed as follows:

$$\lambda = \frac{2\pi}{\omega\sqrt{L \cdot C}}, \tag{A-13}$$

A.3. Expressions of the EM Fields Radiated by the Cable

It was demonstrated that the electric field components radiated by the structure presented in Fig. A.1 are expressed as:

$$E_x = 0, \tag{A-14}$$

$$E_y = 8K \frac{y \cdot z \cdot u}{[y^2 + (z+u)^2][y^2 + (z-u)^2]}, \tag{A-15}$$

$$E_z = 4K \frac{h(y^2 - z^2 + u^2)}{[y^2 + (z+u)^2][y^2 + (z-u)^2]}, \tag{A-16}$$

where

$$K = \frac{\sqrt{2P \cdot Z_c}}{\ln\left(\frac{h+u}{h-u}\right)}, \tag{A-17}$$

and

$$u = \sqrt{h^2 - a^2}\ . \tag{A-18}$$

By considering the characteristic impedance of the medium defined in (A-9), the magnetic field components are written as:

$$H_x = 0, \tag{A-19}$$

$$H_y = -\frac{E_z}{Z_c}, \tag{A-20}$$

$$H_z = -\frac{E_y}{Z_c}. \tag{A-21}$$

ACKNOWLEDGEMENTS

These research works is within the frame of the “Time Domain Electromagnetic Characterization and Simulation for EMC” (TECS) project which is part-funded by the Haute-Normandie Region (FRANCE) and the ERDF via the Franco-British Interreg IVA European programme No 4081.

REFERENCES

[1]. T. Yang, Y. Bayram & J. L. Volakis, (2010) “Hybrid analysis of electromagnetic interference effects on microwave active circuits within cavity enclosures,” *IEEE Trans. EMC*, Vol. 52, No. 3, pp. 745-748.

[2]. D. Vye, (2011) “EMI by the dashboard light,” *Microwave Journal*, Vol. 54, No. 7, pp. 20-23.

[3]. T. Hubing, (2011) “Ensuring the Electromagnetic Compatibility of Safety Critical Automotive Systems,” *Proc. of Invited Plenary Speaker at the 2011 APEMC*, Jeju, S. Korea.

[4]. M. Wiles, (2003) “An Overview of Automotive EMC Testing Facilities,” *Automotive EMC Conference 2003, Milton Keynes, UK*.

[5]. J. Shin, (2011) “Automotive EMC Standards and Testing,” *Proc. of Tutorial Workshop Digests on “Introduction to Automotive EMC Testing” at the 2011 APEMC*, Jeju, S. Korea.

[6]. K. Liu, (2011) “An Update on Automotive EMC Testing,” *Microwave Journal*, Vol. 54, No. 7, pp. 40-46.

[7]. R. De Leo, V. Mariani & V. Vespasian, (2001) “Characterization of automotive battery in the RF range for EMC application”, *Proc. of 14th Int. EMC Zurich Symp.*, Zurich, Switzerland.

[8]. S. Chen, T.W. Nehl, J.-S. Lai, X. Huang, E. Pepa, R. De Doncker & I. Voss, (2003) “Towards EMI prediction of a PM motor drive for automotive applications,” *Proc. of 18th Annual IEEE Applied Power Electronics Conference and Exposition*, *APEC’03*, Orlando, FL, USA, Vol. 1, pp. 14-22.

[9]. C.-N. Chiu & C.-C. Yang, (2010) "A solution for increasing immunity against the influence of ground variations on a board integrated GPS antenna", *PIER C*, Vol. 15, pp. 211-218.

[10]. H. Xie, J. Wang, R. Fan, & Y. Liu, (2010) "Spice Models for Radiated and Conducted Susceptibility Analyses of Multiconductor Shielded Cables," *PIER* 103, pp. 241-257.

[11]. P. Fernandez Lopez, A. Ramanujan, Y. Vives Gilabert, C. Arcambal, A. Louis, & B. Mazari, (2009) "A radiated emission model compatible to a commercial electromagnetic simulation tool," *Proc. of 20th Int. EMC Zurich Symp.*, pp. 369-372, Zurich, Switzerland.

[12]. A. Ramanujan, Z. Riah, A. Louis, & B. Mazari, (2010) "Modeling the electromagnetic radiation of passive microwave components using a near-field scanning method," *IEEE Trans. EMC*, Vol. 52, No. 4, pp. 1056-1059.

[13]. L. Paletta, J. P. Parmantier, F. Issac, P. Dumas & J. C. Alliot, (2002) "Susceptibility analysis of wiring in a complex system combining a 3-D solver and a transmission-line network simulation," *IEEE Trans. EMC*, Vol. 44, No. 2, pp. 309-317.

[14]. C. D. Taylor, R. S. Sattewhite, & C. W. Harrison, (1965) "The response of a terminated two-wire transmission line excited by a nonuniform electromagnetic field," *IEEE Trans. Ant. Propagat*., Vol. 13, No. 6, pp. 987-989.

[15]. A. K. Agrawal & H. J. Price, (1980) "Transient response of multiconductor transmission lines excited by a non uniform electromagnetic field," *IEEE Trans. Ant. Prop.*, Vol. 18, pp. 432- 435.

[16]. F. Rachidi, (1993) "Formulation of the field to transmission line coupling equations in terms of magnetic excitation field", *IEEE Trans. EMC*, Vol. 35, No. 3, pp. 404-407.

[17]. S. Atrous, D. Baudry, E. Gaboriaud, A. Louis, B. Mazari & D. Blavette, (2008) "Near-field investigation of the radiated susceptibility of printed circuit boards," *Int. Symp. on EMC Europe*, Hamburg, Germany.

[18]. C. Leseigneur, P. F. Lopez, C. Arcambal, D. Baudry & A. Louis, (2010) "Near-field coupling model between electronic systems and transmission line," *IEEE Int. Symp. EMC*, Fort Lauderdale, FL, USA, pp. 22-27.

[19]. E. R. Rajkumar, B. Ravelo, M. Bensetti, & P. Fernandez-Lopez, (2012) "Application of a hybrid model for the susceptibility of arbitrary shape electric wires disturbed by EM near-field radiated by electronic structures," *PIER B* 37, pp. 143-169.

[20]. E. R. Rajkumar, A. Ramanujan, M. Bensetti, B. Ravelo & A. Louis, (2011) "Comparison between Hybrid Methods in the Optimization of Radiated Coupling Calculation," *Proc. of 5th ICONIC 2011*, Rouen, France.

[21]. E. R. Rajkumar, M. Bensetti, B. Ravelo, A. Ramanujan & A. Louis, (2012) "Cable immunity analysis with 2D/3D-dipoles near-field radiation", Submitted for communication to Advanced Electromagnetics Symposium (AES) 2012, Paris, France.

[22]. E. R. Rajkumar, M. Bensetti, B. Ravelo, A. Ramanujan & A. Louis, (2012) "Improvised PEEC method in the modelling of the near-field coupling with electrical cable*", (Accepted for communication) Proc. of PIERS*, Kuala Lumpur, Malaysia.

[23]. E. Rajkumar, A. Ramanujan, B. Ravelo & M. Bensetti, (2012) "A hybrid technique for radiated coupling exposed to near- and far-fields", (Submitted) *Proc. of the 16ème Colloque international sur la compatibilité électromagnétique* (*CEM*) *2012*, Rouen, France.

[24]. B. Ravelo, Y. Liu, A. Louis & A. K. Jastrzebski, (2011) "Study of high-frequency electromagnetic transients radiated by electric dipoles in near-field," *IET Microw. Antennas Propag*., Vol. 5, No, 6, pp 692 - 698.

[25]. B. Ravelo, Z. Riah, D. Baudry & B. Mazari, (2011) "E-field extraction from Hx- and Hy- near field values by using plane wave spectrum method," *Eur. Phys. J. Appl. Phys.*, Vol. 53, No. 1, 11201-pp. 1-10.

Authors' biography

Elagiri Ramalingam Rajkumar was born in India. He has completed his Ph.D Degree in electronics (EMC/EMI) from university of Rouen,Rouen,France in 2012.Earlier he completed his B.E (ECE), M.Tech (BME) degrees from Madras University and VIT University, T.N, India, respectively. He has been working as Research Engineer and Visiting Researcher in France from 2008. From 2000 to 2008 during his tenure at VIT University, India, he was part of the new department creation and university development activities. He has 15 years of experience of teaching and research experiences in India and aboard. His research interests include hybrid methods, EMC/EMI, and neural imaging and Bioelectromagnetics and intelligent transport systems.

Blaise Ravelo is currently assistant professor on electronic circuit theory, telecommunication science & technology and microwave/digital engineering. He is the pioneer of the negative group delay (NGD) microwave active circuit development using transistor. His research interest is mainly focused on the applications of NGD circuits for the microwave/digital microelectronic systems signal integrity (SI) and the characterization of the transient EMC/EMI radiation emission and immunity. He is (co-) author of nineties papers published in international journals, books and conference proceedings. He is regularly reviewer of papers submitted to int. journals (IEEE Trans. MTT/CAS/EMC, JEWMA, Int. J. of Electronic, JEEER, PIER, Intech Book…).

Mohamed Bensetti received his Master's Research degree (DEA) in 2001 and his Ph.D. in Electrical Engineering in 2004 from the University of Paris XI, France. From 2005 to 2007, he worked as a researcher in Ecole superieure d'Electricité (SUPELEC) – Gif-Sur-Yvette - France. Since 2007, he has joined the Graduate Engineering School ESIGELEC, Rouen, where he is lecturer and researcher in the Research Institute for Electronic Embedded Systems (IRSEEM). His domains of research are ElectroMagnetic Compatibility (EMC) and Power Electronics including modelling, simulation and neural networks.

Yang Liu was born in Dalian (China) in 1982. He received his master's degree in electronic and communication system from Pierre and Marie CURIE University (UPMC) in 2009. At present, he works at IRSEEM (Institute of research on embedded electronic system) laboratory as a PhD student. His research interests include near-field characterization and measurement for EMC application in time domain, electromagnetic simulation and modeling.

Priscilla Fernández López was born in Oviedo, Spain, in 1982. She received the degree in telecommunication engineering from the University of Oviedo, Gijón, Spain, in 2007 and the Ph.D. degree in electronics at the University of Rouen, Mont Saint Aignan, France, in 2011. From 2006 to 2011, she was a researcher in IRSEEM. Her research activities included electromagnetic compatibility (EMC), particularly the measurement and modelling of radiated emissions of electronic components. She is currently with Valeo, Créteil, France, where she is working on the EMC aspects for automotive applications.

Fabrice Duval was born in Normandy. He received the Ph.D degree in electronic engineering from the University of Paris XI, France, in 2007. He is currently the head of EMC laboratory of IRSEEM/ ESIGELEC in Rouen, France. His main research activity is EMC modeling for large systems (automotives and aeronautics) in order to produce new tools and models of wires, MOS, passive components.

Moncef Kadi was born in Constantine, Algeria, in March 17, 1974. He received the Electr. Eng. Dipl. from the University of Constantine, Constantine, in 1996, the Master's Research degree (D.E.A) in Optoelectronic, optics and microwaves from the National Polytechnic Institute of Grenoble (INPG), Grenoble, France, in 2001, and the Ph.D. degree in RF and Optics from the University Joseph Fourier, Grenoble, in 2004. In October 2004 he joined the Research Institute for Embedded systems (IRSEEM), Ecole Supérieure d'Ingénieurs (ESIGELEC), Rouen, France, as a Postdoctoral Fellow, and is currently a lecturer/researcher and a head of electronic and system research group. His current research interests include the area of electromagnetic compatibility, antennas design, probe characterization, and susceptibility of integrated circuits.